

Chiral Organometallic Triangles with Rh–Rh Bonds. 1. Compounds Prepared from Racemic *cis*-Rh₂(C₆H₄PPh₂)₂(OAc)₂

F. Albert Cotton,* Carlos A. Murillo,* Xiaoping Wang, and Rongmin Yu

Department of Chemistry and the Laboratory for Molecular Structure and Bonding,
P.O. Box 3012, Texas A&M University, College Station, Texas 77842-3012

Received June 16, 2004

Reaction of racemic *cis*-Rh₂(C₆H₄PPh₂)₂(OAc)₂(HOAc)₂ with excess Me₃OBF₄ in CH₃CN results in the formation of racemic *cis*-[Rh₂(C₆H₄PPh₂)₂(CH₃CN)₆](BF₄)₂·0.5H₂O (1·0.5H₂O), an ionic dirhodium complex which has two cisoid nonlabile orthometalated phosphine bridging anions and six labile CH₃CN ligands in equatorial and axial positions. Reactions of **1** with tetraethylammonium salts of the linear dicarboxylates, oxalate, terephthalate, and 4,4'-biphenyldicarboxylate, in organic solvents, produced racemic crystals of the triangular compounds [Rh₂(C₆H₄PPh₂)₂]₃(C₂O₄)₃·(py)₆·6MeOH·H₂O (**2**·6MeOH·H₂O), [Rh₂(C₆H₄PPh₂)₂]₃(O₂CC₆H₄CO₂)₃(DMF)₆·6.5DMF·0.5H₂O (**3**·6.5DMF·0.5H₂O), and [Rh₂(C₆H₄PPh₂)₂]₃(O₂CC₆H₄C₆H₄CO₂)₃(py)₆·4.5CH₃OH·0.75H₂O (**4**·4.5CH₃OH·0.75H₂O), respectively. All compounds are electrochemically active. The relative chiralities of the dirhodium units in each triangle have been established using a combination of data from X-ray crystallography and ³¹P NMR spectroscopy.

Introduction

The designed, convergent synthesis of inorganic and organometallic macrocycles, driven by metal–ligand interactions, and study of those products have become topics of great interest in supramolecular chemistry.¹ In early work, mononuclear units, such as M(amine)_n²⁺ (M = Pd, Pt, Zn and *n* = 1 or 2) were used to construct many supramolecular architectures such as triangles, squares, and other polygons, as well as helices and 2-D or 3-D structures.² Important limitations of this earlier work are that the majority of these entities are nonmagnetic and carry high positive charges, and the metal ions mainly used (Pd²⁺, Pt²⁺, Zn²⁺) do not allow for alteration of oxidation states by electrochemical or other means without collapse of the structures. Furthermore, the metal centers are usually coordinatively saturated, which obviates applications such as metal-based catalysis or use

of the metal centers to form more complex structures through further coordination chemistry.

In this laboratory, the use of appropriately designed dimetal units (e.g., Mo₂⁴⁺ and Rh₂⁴⁺) to fabricate higher order structures (so-called supramolecules) has been demonstrated.³ These higher order structures include pairs, loops, triangles, squares, tubes, sheets, and three-dimensional structures. Importantly, use of appropriate paddlewheel dimetal units can readily introduce magnetically, electrochemically, and catalytically active metal centers into such molecules.

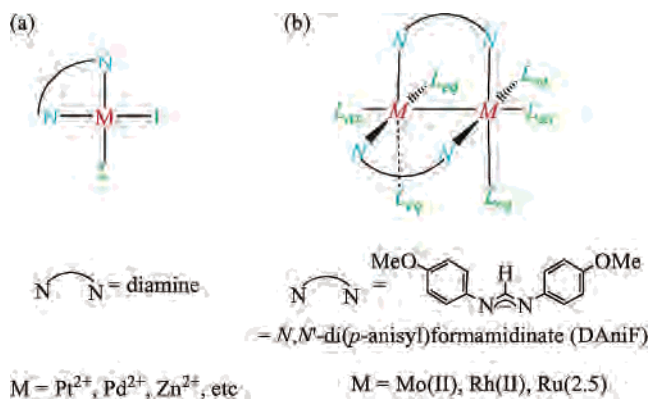
The general structures of the mononuclear and dinuclear building blocks used as precursors to higher order structures are shown in Scheme 1. They contain both spectator (i.e., nonlabile) and labile ligands, with pairs of labile ones oriented approximately 90° to one another. These precursors react generally with linear rigid linkers to produce molecular squares, but occasionally molecular triangles have been observed.⁴ Intentional formation of triangular complexes is less common, and this may be attributed to the scarcity of building blocks with ligands having angles of 60°.⁵ Only three triangles, [Rh₂(*cis*-DAniF)₂](O₂CCO₂)₃, [Mo₂(*cis*-DAniF)₂](*trans*-1,4-O₂CC₆H₁₀CO₂)₃ (DAniF = *N,N'*-(di-*p*-anisyl)formamidinate), and Re₂Cl₂(dppm)₂]₃(O₂CC₆H₄CO₂)₃, have been previously reported from the well-known paddle-

* To whom correspondence should be addressed. E-mail: cotton@tamu.edu (F.A.C.); murillo@tamu.edu (C.A.M.).

(1) Lehn, J.-M. *Supramolecular Chemistry: Concepts and Perspectives*; VCH: New York, 1995.
(2) (a) Seidel, S. R.; Stang, P. J. *Acc. Chem. Res.* **2002**, *35*, 972. (b) Swiegler, G. F.; Malefetse, T. J. *Coord. Chem. Rev.* **2002**, *225*, 91. (c) Holliday, B. J.; Mirkin, C. A. *Angew. Chem., Int. Ed.* **2001**, *40*, 2022. (d) Leininger, S.; Olenyuk, B.; Stang, P. J. *Chem. Rev.* **2000**, *100*, 853. (e) Fujita, M. *Chem. Soc. Rev.* **1998**, *27*, 417. (f) Onisuka, K.; Yamamoto, S.; Takahashi, S. *Angew. Chem., Int. Ed.* **1999**, *38*, 174. (g) Slone, R. V.; Benkstein, K. D.; Bélanger, S.; Hupp, J. T.; Guzei, I. A.; Rheingold, A. L. *Coord. Chem. Rev.* **1998**, *171*, 221.

(3) (a) Cotton, F. A.; Lin, C.; Murillo, C. A. *Acc. Chem. Res.* **2001**, *34*, 759. (b) Cotton, F. A.; Lin, C.; Murillo, C. A. *Proc. Natl. Acad. Sci. U.S.A.* **2002**, *99*, 4810.

Scheme 1



wheel building blocks of type b, Scheme 1, where labile axial ligands may or may not be present.⁶

It must be borne in mind that there is an entropic preference for the formation of $n/3$ moles of triangles rather than $n/4$ moles of squares from a mixture of n moles of angular corner pieces and n moles of linkers. However, if the corner pieces are fragments of a paddlewheel in which adjacent edges (at 90°) are to be used and the linkers are rigid, linear dicarboxylates, the entropic factor is likely to lose out to the enthalpic one that arises from the directional preferences of the components. In the triangle obtained by combining $cis\text{-Mo}_2(\text{DAniF})_2^{2+}$ units and cyclohexane 1,4-dicarboxylate,^{6b} the factor that allows the entropic factor to dominate is the ease with which the dicarboxylate can bend so that the 90° angle at the dimolybdenum corner pieces can be accommodated in the triangle.

It is especially relevant to the work reported here that in a reaction intended to produce only the square compound $[\text{Rh}_2(cis\text{-DAniF})_2(\text{O}_2\text{CCO}_2)]_4$, it was found that either squares or triangles can be made in quantitative yields by adjusting the reaction conditions.^{6a} Formation of this triangle is believed to be due in part to the rotational flexibility of

the single bond in the Rh_2^{4+} units, which has no inherent resistance to moderate twisting about the Rh–Rh axis, since there is only a net σ bond with a $\sigma^2\pi^4\delta^2\delta^2\pi^*4$ configuration. Such twisting reduces some of the strain in the triangle. However, attempts to make more triangles using the $cis\text{-Rh}_2(\text{DAniF})_2^{2+}$ unit and other rigid linear ligands, such as terephthalate, perfluoroterephthalate, and fumarate, were not successful, and all of the subsequently isolated higher order structures have been molecular squares.⁷ In other reactions of suitable Rh_2^{4+} units and rigid linear dicarboxylate linkers, only molecular squares have been obtained.⁸

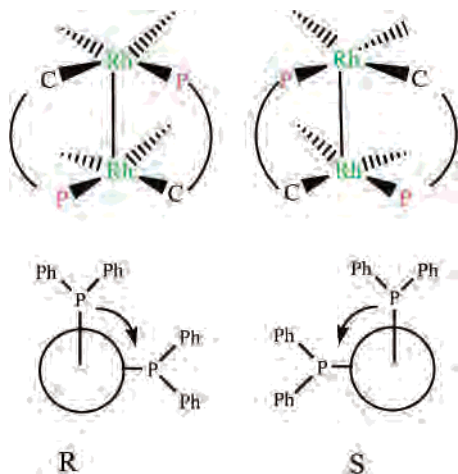
Another important theme in the area of transition-metal-based supramolecular compounds is the incorporation of chirality with the goal of endowing the products with enantioselectivity in their reactivity toward substrates.^{9,10} There are several general ways to assemble higher-order structures that are chiral: (1) by using chiral linkers; (2) by attaching chiral spectator ligands to the metal corner pieces. The use of chiral linkers has been implemented several times with single-metal-atom corners,^{4e,f,11} and on a few occasions with the dinuclear units $cis\text{-Mo}_2(\text{DAniF})_2^{2+}$ ¹² and $\text{Ru}_2(\text{CO})_4(\text{L}_{ax})_2^{2+}$.¹³

A third important concept that could be useful for the introduction of chirality to supramolecules, that has not been generally employed, is the use of inherent chirality of certain single metal centers where the ligands are not chiral themselves.¹⁴ Examples are afforded by the formation of racemic mixtures of triangular macrocycles in which half-sandwich complexes of iridium(III) and ruthenium(II) occupy corner positions¹⁵ and by the racemic crystals of a triangle having cobalt atoms.¹⁶ Very large hexagons have also been described using Δ and Λ tris-chelate complexes as corner pieces.¹⁷

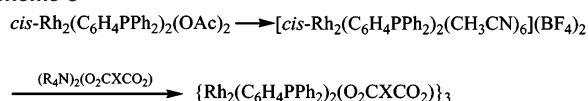
- (4) See for example: (a) Mukherjee, P. S.; Das, N.; Kryschenko, Y. K.; Arif, A. M.; Stang, P. J. *J. Am. Chem. Soc.* **2004**, *126*, 2464. (b) Lehaire, M.-L.; Scopelliti, R.; Herdeis, L.; Polborn, K.; Mayer, P.; Severin, K. *Inorg. Chem.* **2004**, *43*, 1609. (c) Kryschenko, Y. K.; Seidel, S. R.; Arif, A. M.; Stang, P. J. *J. Am. Chem. Soc.* **2003**, *125*, 5193. (d) Ferrer, M.; Mounir, M.; Rossell, O.; Ruiz, E.; Maestro, M. A. *Inorg. Chem.* **2003**, *42*, 5890. (e) Jiang, H.; Lin, W. *J. Am. Chem. Soc.* **2003**, *125*, 8084. (f) Lee, S. J.; Hu, A.; Lin, W. *J. Am. Chem. Soc.* **2002**, *124*, 12948. (g) Schweiger, M.; Seidel, S. R.; Arif, A. M.; Stang, P. J. *Inorg. Chem.* **2002**, *41*, 2556. (h) Piotrowski, H.; Polborn, K.; Hilt, G.; Severin, K. *J. Am. Chem. Soc.* **2001**, *123*, 2699. (i) Schweiger, M.; Seidel, S. R.; Arif, A. M.; Stang, P. J. *Angew. Chem., Int. Ed.* **2001**, *40*, 3467. (j) Sautter, A.; Schmid, D. G.; Jung, G.; Würthner, F. *J. Am. Chem. Soc.* **2001**, *123*, 5424. (k) Schnebeck, R.-D.; Freisinger, E.; Glahé, F.; Lippert, B. *J. Am. Chem. Soc.* **2000**, *122*, 1381. (l) Sun, S.-S.; Lees, A. J. *J. Am. Chem. Soc.* **2000**, *122*, 8956. (m) Lai, S.-W.; Chan, M. C.-W.; Peng, S.-M.; Che, C.-M. *Angew. Chem., Int. Ed.* **1999**, *38*, 669. (n) Schnebeck, R.-D.; Freisinger, E.; Lippert, B. *Angew. Chem., Int. Ed.* **1999**, *38*, 168. (o) Whang, D.; Park, K.-M.; Heo, J.; Ashton, P.; Kim, K. *J. Am. Chem. Soc.* **1998**, *120*, 4899. (p) Hall, J. R.; Loeb, S. J.; Shimizu, G. K. H.; Yap, G. P. A. *Angew. Chem., Int. Ed.* **1998**, *37*, 121.
- (5) Olenyuk, B.; Fechtenkötter, A.; Stang, P. J. *J. Chem. Soc., Dalton Trans.* **1998**, 1707.
- (6) (a) Cotton, F. A.; Daniels, L. D.; Lin, C.; Murillo, C. A. *J. Am. Chem. Soc.* **1999**, *121*, 4538. (b) Cotton, F. A.; Lin, C.; Murillo, C. A. *Inorg. Chem.* **2001**, *40*, 575. (c) Bera, J. K.; Angaridis, P.; Cotton, F. A.; Petrukhina, M. A.; Fanwick, P. E.; Walton, R. A. *J. Am. Chem. Soc.* **2001**, *123*, 1515.

- (7) Cotton, F. A.; Daniels, L. M.; Lin, C.; Murillo, C. A.; Yu, S.-Y. *J. Chem. Soc., Dalton Trans.* **2001**, 502.
- (8) (a) Bickley, J. F.; Bonar-Law, R. P.; Femoni, C.; MacLean, E. J.; Steiner, A.; Teat, S. J. *J. Chem. Soc., Dalton Trans.* **2000**, 4025. (b) Bonar-Law, R. P.; McGrath, T. G.; Singh, N.; Bickley, J. F.; Steiner, A. *Chem. Commun.* **1999**, 2457.
- (9) Doyle, M. P.; McKervey, M. A.; Ye, T. *Modern Catalytic Methods for Organic Synthesis with Diazo Compounds*; John Wiley & Sons: New York, 1998.
- (10) (a) Barberis, M.; Pérez-Prieto, J.; Herbst, K.; Lahuerta, P. *Organometallics* **2002**, *21*, 1667. (b) Estevan, F.; Herbst, K.; Lahuerta, P.; Barberis, M.; Pérez-Prieto, J. *Organometallics* **2001**, *20*, 950. (c) Barberis, M.; Lahuerta, P.; Pérez-Prieto, J.; Sanaú, M. *Chem. Commun.* **2001**, 439. (d) Estevan, F.; Lahuerta, P.; Pérez-Prieto, J.; Pereira, I.; Stiriba, S.-E. *Organometallics* **1998**, *17*, 3442. (e) Estevan, F.; Lahuerta, P.; Pérez-Prieto, J.; Sanaú, M.; Stiriba, S.-E.; Ubeda, A. M. *Organometallics* **1997**, *16*, 880.
- (11) (a) Lee, S. J.; Lin, W. *J. Am. Chem. Soc.* **2002**, *124*, 4554. (b) Lee, S. J.; Luman, C. R.; Castellano, F. N.; Lin, W. *Chem. Commun.* **2003**, 2124. (c) Hu, A.; Ngo, H. L.; Lin, W. *J. Am. Chem. Soc.* **2003**, *125*, 11490.
- (12) (a) Cotton, F. A.; Donahue, J. P.; Murillo, C. A. *Inorg. Chem. Commun.* **2002**, *5*, 59. (b) Berry, J. F.; Cotton, F. A.; Ibragimov, S. A.; Murillo, C. A.; Wang, X. *Dalton Trans.* **2003**, 4297.
- (13) Süß-Fink, G.; Wolfender, J.-L.; Neumann, F.; Stoeckli-Evans, H. *Angew. Chem., Int. Ed. Engl.* **1990**, *29*, 429.
- (14) For reviews of chirality at metal centers, see for example: (a) Keene, F. R. *Coord. Chem. Rev.* **1997**, *166*, 121. (b) Knof, U.; von Zelewsky, A. *Angew. Chem., Int. Ed.* **1999**, *38*, 303.
- (15) Haberer, T.; Warchhold, M.; Nöth, H.; Severin, K. *Angew. Chem., Int. Ed.* **1999**, *38*, 3225.
- (16) Dreos, R.; Nardin, G.; Randaccio, L.; Siega, P.; Tauzher, G. *Eur. J. Inorg. Chem.* **2002**, 2885.
- (17) Ali, Md. M.; MacDonnell, F. M. *J. Am. Chem. Soc.* **2000**, *122*, 11527.

Scheme 2



Scheme 3



We report here for the first time the use of an inherently chiral metal–metal bonded unit. We do this by employing the building block $cis\text{-Rh}_2(\text{C}_6\text{H}_4\text{PPh}_2)_2^{2+}$, shown in Scheme 2 in each of the *R* and *S* enantiomeric forms (vide infra).¹⁸ The initial source of this building block is $cis\text{-Rh}_2(\text{C}_6\text{H}_4\text{PPh}_2)_2(\text{OAc})_2(\text{HOAc})_2$, a compound that is easily prepared as a racemate.¹⁹ In practice, we find that it is best if this acetate compound is first converted to $[cis\text{-Rh}_2(\text{C}_6\text{H}_4\text{PPh}_2)_2(\text{CH}_3\text{CN})_6](\text{BF}_4)_2$ (**1**), which then reacts smoothly with the dicarboxylate linkers to afford triangles (Scheme 3). As will be seen, the only supramolecular products obtained in the work reported here are triangles. We shall discuss the reason for this following the Experimental Section.

By using racemic starting materials, one would expect to obtain racemic products, and that is what we report here. In a future report, we shall describe the results of using resolved enantiomers of the same starting material in otherwise similar reactions.

Experimental Section

Materials and Methods. Unless otherwise stated, all manipulations and procedures were conducted in air. Solvents were used directly as received. Tetraethylammonium salts of dicarboxylic acids were prepared and isolated as colorless solids by neutralization of the corresponding diacids with 2 equiv of 35% aqueous Et_4NOH followed by careful drying under vacuum. All other reagents were purchased from commercial sources and used as received; $cis\text{-Rh}_2(\text{C}_6\text{H}_4\text{PPh}_2)_2(\text{OAc})_2 \cdot 2\text{CH}_3\text{COOH}$ was prepared as reported.¹⁹

Elemental analyses were performed by Canadian Microanalytical Service, Delta, British Columbia, Canada. Because the interstitial molecules and ligands in the axial positions are easily lost and easily exchanged with water molecules in air, the results of the elemental

(18) For a description of the chirality and separation of enantiomers of the parent compound $cis\text{-Rh}_2(\text{C}_6\text{H}_4\text{PPh}_2)_2(\text{OAc})_2$ see: Taber, D. F.; Malcolm, S. C.; Bieger, K.; Lahuerta, P.; Sanau, M.; Stiriba, S.-E.; Pérez-Prieto, J.; Monge, M. A. *J. Am. Chem. Soc.* **1999**, *121*, 860.

(19) Chakravarty, A. R.; Cotton, F. A.; Tocher, D. A.; Tocher, J. H. *Organometallics* **1985**, *4*, 8.

analyses are fitted using a combination of a variety of axial ligands and solvent molecules. The cyclic voltammograms (CVs) and differential pulse voltammograms (DPVs) were taken using a CH Instruments model-CHI 620A electrochemical analyzer in a 0.1 M Bu_4NPF_6 solution in CH_2Cl_2 with Pt working and auxiliary electrodes, a Ag/AgCl reference electrode, and a scan rate of 0.1 V/s for CV and 0.004 V/s for DPV. All the potential values are referenced to the Ag/AgCl electrode, and under the present experimental conditions, the $E_{1/2}$ for the Fc^+/Fc couple consistently occurred at 440 mV. Spectra, ^1H NMR (using the residual proton of the deuterated solvent CD_2Cl_2 or CDCl_3 as reference) and $^{31}\text{P}\{^1\text{H}\}$ NMR (using H_3PO_4 in CDCl_3 as reference), were recorded on a Mercury-300 NMR spectrometer. Mass spectroscopic data (electrospray ionization) were recorded at the Laboratory for Biological Mass Spectrometry at Texas A&M using an MDS Series Qstar Pulsar spectrometer with a spray voltage of 5 keV, and using CH_2Cl_2 or CH_3CN solutions.

Preparation of $cis\text{-}[\text{Rh}_2(\text{C}_6\text{H}_4\text{PPh}_2)_2(\text{CH}_3\text{CN})_6](\text{BF}_4)_2 \cdot 0.5\text{H}_2\text{O}$ (1**·**0.5H₂O**).** A mixture of $cis\text{-Rh}_2(\text{C}_6\text{H}_4\text{PPh}_2)_2(\text{OAc})_2 \cdot 2\text{CH}_3\text{COOH}$ (330 mg, 0.340 mmol) and Me_3OBF_4 (330 mg, 2.14 mmol) in 10 mL of CH_3CN was stirred for 30 min forming a red solution. After removal of the solvent, the residue was washed with 3×10 mL portions of Et_2O , and then dissolved in 6 mL of CH_3CN . Upon addition of a layer of Et_2O , red crystals formed. Yield: 303 mg, 75%. ^1H NMR (in CD_2Cl_2 , δ , ppm): 7.787 (t, 4H, C_6H_5), 7.553 (m, 6H, C_6H_5), 7.319 (t, 2H, C_6H_4), 7.122 (dt, 4H, C_6H_5), 6.753 (m, 8H, C_6H_4 and C_6H_5), 6.639 (t, 2H, C_6H_4), 6.358 (dd, 2H, C_6H_4), 2.065 (s, 18H, CH_3CN). $^{31}\text{P}\{^1\text{H}\}$ NMR (ppm in CD_3CN): 25.77 (d, $^1J_{\text{PRh}} = 148.8$ Hz). Anal. Calcd for $\text{C}_{47}\text{H}_{45.5}\text{B}_2\text{F}_8\text{N}_{5.5}\text{O}_{0.5}\text{P}_2\text{Rh}_2(\text{Rh}_2(\text{C}_6\text{H}_4\text{PPh}_2)_2(\text{CH}_3\text{CN})_{5.5}(\text{BF}_4)_2 \cdot 0.5\text{H}_2\text{O})$: C, 49.66; H, 4.03; N, 6.78%. Found: C, 49.56; H, 4.04; N, 6.64%.

Preparation of $[\text{Rh}_2(\text{C}_6\text{H}_4\text{PPh}_2)_2]_3(\text{C}_2\text{O}_4)_3(\text{py})_6 \cdot 6\text{MeOH} \cdot \text{H}_2\text{O}$ (2**·**6MeOH**·**H₂O**).** A red solution of **1** (38 mg, 0.033 mmol) and $(\text{Et}_4\text{N})_2\text{C}_2\text{O}_4$ (12 mg, 0.034 mmol) in a mixture of 5 mL of CH_2Cl_2 and 0.5 mL of pyridine was layered with 25 mL of methanol. A red crystalline solid was isolated after 5 days, and then dissolved in a mixture of solvents containing 4 mL of CH_2Cl_2 and 1 mL of pyridine. Diffraction quality crystals of the product were obtained by layering isomeric hexanes over a CH_2Cl_2 solution for a period of 10 days. Yield: 23 mg, 66%. ^1H NMR (δ , ppm in CDCl_3): 8.747 (d, 12H, pyridine), 7.597 (t, 6H, pyridine), 6.332–7.174 (m, 96H, aromatic + others from py). $^{31}\text{P}\{^1\text{H}\}$ NMR (ppm in CDCl_3): 19.15 (d, $^1J_{\text{PRh}} = 170.3$ Hz). Anal. Calcd for $\text{C}_{147}\text{H}_{128}\text{N}_6\text{O}_{16}\text{P}_6\text{Rh}_6(\text{Rh}_6(\text{C}_6\text{H}_4\text{PPh}_2)_6(\text{C}_2\text{O}_4)_3(\text{py})_6(\text{MeOH})_3 \cdot (\text{H}_2\text{O}))$: C 58.11, H 4.25, N 2.77%. Found: C 57.99, H 3.92, N 2.78%.

Preparation of $[\text{Rh}_2(\text{C}_6\text{H}_4\text{PPh}_2)_2]_3(\text{O}_2\text{CC}_6\text{H}_4\text{CO}_2)_3(\text{DMF})_6 \cdot 6.5\text{DMF} \cdot 0.5\text{H}_2\text{O}$ (3**·**6.5DMF**·**0.5H₂O**).** A mixture of **1** (88 mg, 0.076 mmol) and $(\text{Et}_4\text{N})_2(\text{O}_2\text{C}_6\text{H}_4\text{CO}_2)$ (48 mg, 0.11 mmol) in 10 mL of CH_3CN was stirred for 10 min at 20 °C, producing a light orange precipitate. The solid was isolated by filtration, washed with 2×10 mL of ether, and dried in air. To the solid was added 5 mL of CH_2Cl_2 and 0.5 mL of DMF. After filtration, the filtrate was allowed to evaporate under a slow stream of nitrogen, affording dark-purple crystals. Yield: 70 mg, 74%. ^1H NMR (ppm in CD_2Cl_2): 7.991 (s, 6H, $\text{H}-\text{C}=\text{O}$ of DMF), 6.567–7.661 (m, 96H, aromatic), 2.978 (s, 18H, CH_3 of DMF), 2.941 (s, 18H, CH_3 of DMF). $^{31}\text{P}\{^1\text{H}\}$ NMR (ppm, in CDCl_3 and DMF): 20.96 (d, $^1J_{\text{PRh}} = 165.3$ Hz), 20.64 (d, $^1J_{\text{PRh}} = 165.8$ Hz), 20.21 (d, $^1J_{\text{PRh}} = 166.2$ Hz). Anal. Calcd for $\text{C}_{144}\text{H}_{138}\text{N}_4\text{O}_{20}\text{P}_6\text{Rh}_6(\text{Rh}_6(\text{C}_6\text{H}_4\text{PPh}_2)_6(\text{C}_8\text{H}_4\text{O}_4)_3 \cdot (\text{DMF})_4(\text{H}_2\text{O})_4)$: C 56.86, H 4.37, N 1.84%. Found: C 56.70, H 4.17, N 1.90%.

Preparation of $[\text{Rh}_2(\text{C}_6\text{H}_4\text{PPh}_2)_2]_3(\text{O}_2\text{CC}_6\text{H}_4\text{C}_6\text{H}_4\text{CO}_2)_3(\text{py})_6 \cdot 4.5\text{CH}_3\text{OH} \cdot 0.75\text{H}_2\text{O}$ (4**·**4.5CH₃OH**·**0.75H₂O**).** A mixture of **1** (30

mg, 0.026 mmol), $(\text{Bu}_4\text{N})_2(\text{O}_2\text{CC}_6\text{H}_4\text{C}_6\text{H}_4\text{CO}_2)$ (22 mg, 0.031 mmol) in CH_2Cl_2 (5 mL), CH_3OH (1 mL), and 5 drops of pyridine was stirred for 15 min. After filtration, the red filtrate was carefully layered with 15 mL of CH_3OH . A crystalline product was isolated after 10 days. Yield: 18 mg, 60%. ^1H NMR (δ , ppm, in CDCl_3): 8.698 (d, 12H, pyridine), 7.744 (t, 6H, pyridine), 6.400–7.480 (m, 120H, aromatic + others from py). ^{31}P $\{^1\text{H}\}$ NMR (ppm in CDCl_3): 21.07 (d, $^1J_{\text{PRh}} = 163.5$ Hz). Anal. Calcd for $\text{C}_{175}\text{H}_{143}\text{N}_5\text{O}_{17}\text{P}_6\text{Rh}_6$ ($\text{Rh}_6(\text{Ph}_2\text{PC}_6\text{H}_4)_6(\text{C}_{14}\text{H}_8\text{O}_4)_3(\text{py})_5(\text{H}_2\text{O})_5$): C 61.98, H 4.25, N 2.06%. Found: C 61.97, H 4.39, N 1.97%.

X-ray Structure Determinations. Data were collected on a Bruker SMART 100 CCD area detector system. Cell parameters were determined using the program SMART.²⁰ Data reduction and integration were performed with the software package SAINT,²¹ while absorption corrections were applied by using the program SADABS.²² The positions of the Rh atoms were found via direct methods using the program SHELXTL.²³ Subsequent cycles of least-squares refinement followed by difference Fourier syntheses revealed the positions of the remaining non-hydrogen atoms. Hydrogen atoms were added in idealized positions. Non-hydrogen atoms, except those for the interstitial molecules, were refined with anisotropic displacement parameters.

In **1**, the phosphine ligand on one of the *cis*- $\text{Rh}_2(\text{C}_6\text{H}_4\text{PPh}_2)_2(\text{CH}_3\text{-CN})_6^{2+}$ cations is disordered in two positions with an occupancy ratio of 0.669(7) to 0.331(7). One of the BF_4^- anions is also disordered, and it was constrained to tetrahedral geometry. For **2**·6MeOH·1.5H₂O, one of the phenyl rings has two orientations in a ratio of 0.650(9) to 0.350(9). Disorder in interstitial solvent molecules were found in compounds **2** and **3**, and these molecules were refined using distance constraints.

In **4**, the position of each Rh₂ corner is occupied disorderedly by both enantiomers (*R* and *S*). Although the existence of triangular species is unquestionable, the X-ray structure analysis does not provide information on the chirality of the triangle. The axial pyridine ligands also have two orientations with comparable occupancies. The R_1 residuals for the least-squares refinement are over 10%. Unfortunately, repeated attempts to obtain crystals with better diffraction data have not been successful. Therefore, we only report some basic data, e.g., cell parameters and a few distances, but its structure will not be discussed in detail. A figure of one orientation of one molecule is provided as Supporting Information. Cell parameters and refinement results for **1–3** are summarized in Table 1. Selected bond distances, bond angles, and torsion angles about Rh–Rh bonds and about the C–C bonds of the oxalate groups for **1–3** are listed in Tables 2–4, respectively. The corresponding structures and crystal packing patterns are shown in Figures 1–3.

Molecular Mechanics Calculations. The calculations were done using the software package Cerius² 4.6 by Accelrys.²⁴ Minimization and molecular mechanics calculations were performed with the Open Force Field (OFF) program in Cerius², using the Universal Force Field.²⁵ Geometric parameters from the single crystal structure of **1** were used as the starting point for the simulation. Minimization of total energy was carried out by fixing the geometry of the inner

Table 1. Crystallographic Data and Structure Refinement Parameters

	1 ·0.5H ₂ O	2 ·6MeOH·H ₂ O	3 ·6.5DMF·0.5H ₂ O
chemical formula	$\text{C}_{48}\text{H}_{47}\text{B}_2\text{F}_8\text{-N}_6\text{O}_{0.5}\text{P}_2\text{Rh}_2$	$\text{C}_{150}\text{H}_{140}\text{N}_6\text{-O}_{19}\text{P}_6\text{Rh}_6$	$\text{C}_{169.5}\text{H}_{184.5}\text{N}_{12.5}\text{-O}_{25}\text{P}_6\text{Rh}_6$
fw	1157.30	3133.96	3600.08
cryst syst	monoclinic	trigonal	monoclinic
space group	<i>C2/c</i>	<i>P31c</i>	<i>P21/n</i>
<i>a</i> (Å)	22.212(3)	19.1896(4)	18.249(1)
<i>b</i> (Å)	23.185(3)	19.1896(4)	26.539(2)
<i>c</i> (Å)	22.209(3)	21.0249(9)	37.635(2)
α (deg)	90	90	90
β (deg)	119.236(2)	90	100.138(1)
γ (deg)	90	120	90
<i>V</i> (Å ³)	9981(2)	6705.0(3)	17941(2)
<i>Z</i>	8	2	4
<i>d</i> _{calcd} (g cm ⁻³)	1.540	1.552	1.333
μ (Mo K α) (mm ⁻¹)	0.797	0.863	0.658
<i>T</i> , °C	–60	–60	–60
GOF	1.030	1.145	1.079
$R_1,^a wR_2^b$	0.0537, 0.1023	0.0308, 0.0800	0.0876, 0.2213

$$^a R_1 = \frac{\sum |F_o| - |F_c|}{\sum |F_o|}, \quad ^b wR_2 = \frac{[\sum w(F_o^2 - F_c^2)^2] / \sum w(F_o^2)^2}{}^{1/2}, \\ w = 1/[\sigma^2(F_o^2) + (aP)^2 + bP], \quad \text{where } P = [\max(F_o^2 \text{ or } 0) + 2(F_c^2)]/3.$$

Table 2. Selected Interatomic Distances (Å), Angles (deg), and Torsion Angles (deg) for **1**·0.5H₂O

Rh(1)–Rh(1A)	2.655(1)	Rh(1)–N(1)	2.131(5)
Rh(1)–P(1)	2.228(2)	Rh(1)–N(2)	2.127(5)
Rh(1)–C(18A)	2.024(5)	Rh(1)–N(3)	2.202(6)
Rh(2)–Rh(2A)	2.656(1)	Rh(2)–N(4)	2.104(6)
Rh(2)–P(2A)	2.242(3)	Rh(2)–N(5)	2.142(6)
Rh(2)–P(2B)	2.232(7)	Rh(2)–N(6)	2.196(6)
Rh(2)–C(26C)	2.05(1)	Rh(2)–C(26D)	2.01(2)
C(18A)–Rh(1)–N(2)	87.4(2)	P(1)–Rh(1)–Rh(1A)–C(18)	–23.0(2)
N(2)–Rh(1)–N(1)	88.3(2)	N(1)–Rh(1)–Rh(1A)–N(2A)	–32.3(2)
C(18A)–Rh(1)–P(1)	87.6(2)	P(1)–Rh(1)–Rh(1A)–P(1A)	–110.03(8)
N(1)–Rh(1)–P(1)	96.7(1)		
N(3)–Rh(1)–Rh(1A)	172.1(1)	C(18A)–Rh(1)–Rh(1A)–C(18)	64.1(3)
C(26C)–Rh(2)–N(5)	83.9(5)	P(2A)–Rh(2)–Rh(2A)–C(26A)	21.1(5)
C(26D)–Rh(2)–N(5)	95(1)	N(5)–Rh(2)–Rh(2A)–N(4A)	31.7(2)
N(5)–Rh(2)–N(4)	86.1(2)	P(2A)–Rh(2)–Rh(2A)–P(2AA)	116.2(3)
N(4)–Rh(2)–P(2A)	94.5(2)	C(26C)–Rh(2)–Rh(2A)–C(26A)	–74.0(9)
N(4)–Rh(2)–P(2B)	105.0(5)	P(2B)–Rh(2)–Rh(2A)–C(26B)	21(1)
C(26C)–Rh(2)–P(2A)	95.5(5)	P(2B)–Rh(2)–Rh(2A)–P(2BA)	94.4(7)
C(26D)–Rh(2)–P(2B)	75(1)	C(26D)–Rh(2)–Rh(2A)–C(26B)	–52(2)
N(6)–Rh(2)–Rh(2A)	169.9(2)		

Table 3. Selected Interatomic Distances (Å), Angles (deg), and Torsion Angles (deg) for **2**·6MeOH·H₂O

Rh(1)–Rh(1A)	2.5650(5)	Rh(1)–C(2)	2.008(3)
Rh(1)–P(1)	2.212(1)	Rh(1)–O(1)	2.117(2)
Rh(1)–O(2)	2.174(2)	Rh(1)–N(1)	2.288(3)
C(2)–Rh(1)–O(1)	89.0(1)	P(1)–Rh(1)–Rh(1A)–C(2A)	12.7(1)
O(1)–Rh(1)–O(2)	83.86(9)	O(1)–Rh(1)–Rh(1A)–O(2A)	18.99(9)
O(2)–Rh(1)–P(1)	94.28(7)	P(1)–Rh(1)–Rh(1A)–P(1A)	105.31(5)
C(2)–Rh(1)–P(1)	92.9(1)	C(2)–Rh(1)–Rh(1A)–C(2A)	–79.9(2)
N(1)–Rh(1)–Rh(1A)	164.26(8)		

core of the *cis*- $\text{Rh}_2(\text{C}_6\text{H}_4\text{PPh}_2)_2(\text{MeCN})_6^{2+}$ ion with C_2 symmetry, and then varying the torsion angle defined by P–Rh–Rh–C unit from –30 to 25° using 2–5° incremental steps. All aryl groups and the acetonitrile carbon atoms were allowed to rotate freely during the energy minimization process.

Results and Discussion

Syntheses. Carboxylate exchange reactions have previously, though not often, been used for the synthesis of

- (25) (a) Rappe, A. K.; Casewit, C. J.; Colwell, K. S.; Goddard, W. A., III; Skiff, W. M. *J. Am. Chem. Soc.* **1992**, *114*, 10024. (b) Castonguay, L. A.; Rappe, A. K. *J. Am. Chem. Soc.* **1992**, *114*, 5832. (c) Rappe, A. K.; Colwell, K. S. *Inorg. Chem.* **1993**, *32*, 3438.

(20) SMART for Windows NT, Version 5.618; Bruker Advanced X-ray Solutions, Inc.: Madison, WI, 2001.

(21) SAINT. Data Reduction Software. Version 6.36A; Bruker Advanced X-ray Solutions, Inc.: Madison, WI, 2001.

(22) SADABS. Area Detector Absorption and other Corrections Software, Version 2.05; Bruker Advanced X-ray Solutions, Inc.: Madison, WI, 2000.

(23) Sheldrick, G. M. SHELXTL, Version 6.12; Advanced X-ray Solutions, Inc.: Madison, WI, 2002.

(24) Cerius² Forcefield-Based Simulations; Accelrys Inc.: San Diego, CA, 2001.

Table 4. Selected Interatomic Distances (Å), Angles (deg), and Torsion Angles (deg) for $3 \cdot 0.5\text{DMF} \cdot 0.5\text{H}_2\text{O}$

Rh(1)–Rh(2)	2.514(1)	Rh(1)–C(44)	2.02(1)	Rh(3)–O(15)	2.296(9)	Rh(3)–O(3)	2.168(7)
Rh(3)–Rh(4)	2.507(1)	Rh(2)–C(26)	1.98(1)	Rh(4)–O(16)	2.335(9)	Rh(3)–O(9)	2.139(9)
Rh(5)–Rh(6)	2.511(1)	Rh(3)–C(86)	1.99(1)	Rh(5)–O(17)	2.322(9)	Rh(4)–O(4)	2.135(7)
Rh(1)–P(1)	2.208(4)	Rh(4)–C(68)	2.018(9)	Rh(6)–O(18)	2.285(7)	Rh(4)–O(10)	2.166(8)
Rh(2)–P(2)	2.202(3)	Rh(5)–C(128)	2.00(1)	Rh(1)–O(1)	2.173(7)	Rh(5)–O(7)	2.211(8)
Rh(3)–P(3)	2.214(3)	Rh(6)–C(110)	2.01(1)	Rh(1)–O(5)	2.157(8)	Rh(5)–O(11)	2.149(7)
Rh(4)–P(4)	2.199(4)	Rh(1)–O(13)	2.314(8)	Rh(2)–O(2)	2.128(7)	Rh(6)–O(8)	2.132(8)
Rh(5)–P(5)	2.198(3)	Rh(2)–O(14)	2.304(8)	Rh(2)–O(6)	2.170(8)	Rh(6)–O(12)	2.188(7)
Rh(6)–P(6)	2.213(3)						
C(44)–Rh(1)–O(5)	93.7(4)	C(86)–Rh(3)–O(9)	93.6(4)	C(128)–Rh(5)–O(11)		88.9(4)	
O(5)–Rh(1)–O(1)	84.3(3)	O(9)–Rh(3)–O(3)	83.3(3)	C(128)–Rh(5)–P(5)		89.8(3)	
C(44)–Rh(1)–P(1)	88.1(4)	C(86)–Rh(3)–P(3)	86.3(4)	O(11)–Rh(5)–O(7)		83.8(3)	
O(1)–Rh(1)–P(1)	93.9(2)	O(3)–Rh(3)–P(3)	97.0(2)	P(5)–Rh(5)–O(7)		97.5(2)	
O(13)–Rh(1)–Rh(2)	165.9(2)	O(15)–Rh(3)–Rh(4)	167.9(3)	O(17)–Rh(5)–Rh(6)		166.8(2)	
C(26)–Rh(2)–O(2)	90.6(4)	C(68)–Rh(4)–O(4)	92.2(3)	C(110)–Rh(6)–O(8)		94.3(4)	
O(2)–Rh(2)–O(6)	83.9(3)	O(4)–Rh(4)–O(10)	83.1(3)	O(8)–Rh(6)–O(12)		82.4(3)	
C(26)–Rh(2)–P(2)	90.7(3)	C(68)–Rh(4)–P(4)	89.5(3)	C(110)–Rh(6)–P(6)		90.6(3)	
O(6)–Rh(2)–P(2)	94.9(2)	O(10)–Rh(4)–P(4)	95.2(3)	O(12)–Rh(6)–P(6)		92.7(2)	
O(14)–Rh(2)–Rh(1)	165.9(2)	O(16)–Rh(4)–Rh(3)	165.6(2)	O(18)–Rh(6)–Rh(5)		167.7(2)	
P(1)–Rh(1)–Rh(2)–C(26)	–9.4(3)	P(3)–Rh(3)–Rh(4)–C(68)	8.8(3)	P(5)–Rh(5)–Rh(6)–C(110)		–10.0(3)	
C(44)–Rh(1)–Rh(2)–P(2)	–12.0(4)	C(86)–Rh(3)–Rh(4)–P(4)	12.0(4)	C(128)–Rh(5)–Rh(6)–P(6)		–10.9(3)	
O(1)–Rh(1)–Rh(2)–O(2)	–13.3(3)	O(3)–Rh(3)–Rh(4)–O(4)	14.0(3)	O(7)–Rh(5)–Rh(6)–O(8)		–13.7(3)	
O(5)–Rh(1)–Rh(2)–O(6)	–13.6(3)	O(9)–Rh(3)–Rh(4)–O(9)	14.2(3)	O(9)–Rh(3)–Rh(4)–O(9)		–15.1(3)	
P(1)–Rh(1)–Rh(2)–P(2)	–99.9(1)	P(3)–Rh(3)–Rh(4)–P(4)	98.1(1)	P(5)–Rh(5)–Rh(6)–P(6)		–100.6(1)	
C(44)–Rh(1)–Rh(2)–C(26)	78.5(5)	C(86)–Rh(3)–Rh(4)–C(68)	–77.4(4)	C(128)–Rh(5)–Rh(6)–C(110)		79.6(4)	

polygonal higher-order structures from metal–metal bonded species. Examples are the reaction of *cis*- $\text{Ru}_2(\text{DAniF})_2(\text{OAc})_2\text{-Cl}$ and oxalic acid or terephthalic acid to form square molecules.²⁶ A disadvantage is that reactions of this type are somewhat reversible and may be rather slow, so they usually require an excess of the dicarboxylic acid and heating. When this method of carboxylate exchange was attempted for the reaction of *cis*- $\text{Rh}_2(\text{C}_6\text{H}_4\text{PPh}_2)_2(\text{OAc})_2(\text{HOAc})_2$ with dicarboxylic acids, it was found that the excess of acid and the high reaction temperatures caused the formation of insoluble byproducts. Because previous work in our laboratory had shown that dimetal precursors such as *cis*- $[\text{Mo}_2(\text{DAniF})_2(\text{CH}_3\text{CN})_4](\text{BF}_4)_2$ and *cis*- $[\text{Rh}_2(\text{DAniF})_2(\text{CH}_3\text{CN})_6](\text{BF}_4)_2$ can be used to construct macrocyclic supramolecules in high yield,^{6a,b,27} we turned to *cis*- $[\text{Rh}_2(\text{C}_6\text{H}_4\text{PPh}_2)_2(\text{CH}_3\text{CN})_6](\text{BF}_4)_2$ (**1**). In **1**, there are six labile $\text{CH}_3\text{-CN}$ ligands, four of which occupy equatorial positions while the other two are in axial positions.

Compound **1** was synthesized in a straightforward manner, similar to the synthesis of the molybdenum analogue [*cis*- $\text{Mo}_2(\text{DAniF})_2(\text{CH}_3\text{CN})_4](\text{BF}_4)_2$.²⁸ A slurry of *cis*- $\text{Rh}_2(\text{C}_6\text{H}_4\text{PPh}_2)_2(\text{OAc})_2(\text{HOAc})_2$ in anhydrous acetonitrile does not react with Me_3OBF_4 , but in slightly wet acetonitrile, the slurry dissolved quickly to produce a clear red solution. Use of an excess of Me_3OBF_4 is important to replace both of the bridging acetate anions. After removal of the solvent in a vacuum, the solid was washed with ether to remove HBF_4 and the excess of Me_3OBF_4 . This gave an analytically pure orange solid of *cis*- $[\text{Rh}_2(\text{C}_6\text{H}_4\text{PPh}_2)_2(\text{CH}_3\text{CN})_6](\text{BF}_4)_2$, as attested by the NMR spectrum.

The preparation of a triangular compound was accomplished from the reaction of *cis*- $[\text{Rh}_2(\text{C}_6\text{H}_4\text{PPh}_2)_2(\text{CH}_3\text{-CN})_6](\text{BF}_4)_2$ (**1**) with the desired dicarboxylate anion. It is also important, in order to obtain a well-defined product, to carry out this reaction in the presence of a strong donor which can coordinate axially. Reactions of this type took place immediately, leading to the formation of a precipitate or a solution depending on the solvent used. Once isolated, NMR spectra provided evidence of the purity of the crystalline products. Structural characterization of **2–4** revealed their triangular structures. While it might have been expected that from the combination of *cis*- $\text{Rh}_2(\text{C}_6\text{H}_4\text{PPh}_2)_2^{2+}$ units with rigid linear dicarboxylate groups molecular squares might form just as when *cis*- $[\text{Mo}_2(\text{DAniF})_2(\text{CH}_3\text{CN})_4](\text{BF}_4)_2$ ^{3a} and *cis*- $[\text{Rh}_2(\text{DAniF})_2(\text{CH}_3\text{CN})_6](\text{BF}_4)_2$ ⁷ were used as starting materials, all the products obtained in this work were triangles. No modification of the reaction conditions has provided any evidence of the formation for square molecules from **1**. The corner piece *cis*- $\text{Rh}_2(\text{C}_6\text{H}_4\text{PPh}_2)_2$ has a preferred twist of ca. 23° about the Rh–Rh bond (vide infra), and for this reason, there is so little strain in the triangular structure relative to the square structure that the entropic favoring of the smaller ring becomes the controlling thermodynamic factor.

Solid State Structures. Compound **1** crystallizes in the centrosymmetric, monoclinic space group *C2/c*. The asymmetric unit contains two independent half molecules in which twofold axes bisect each Rh–Rh bond. For each molecule, the core is composed of a singly bonded Rh_2^{4+} unit, two bridging orthometalated $\text{C}_6\text{H}_4\text{PPh}_2$ ligands in a cisoid disposition, and six neutral acetonitrile ligands. Four CH_3CN molecules occupy equatorial positions, and two are in axial positions as shown in Figure 1. Thus, each rhodium atom is bonded to a carbon atom and a phosphorus atom, each from a different $\text{C}_6\text{H}_4\text{PPh}_2$ ligand, and also to three nitrogen atoms

(26) Angaridis, P.; Berry, J. B.; Cotton, F. A.; Murillo, C. A. *J. Am. Chem. Soc.* **2003**, *125*, 10327.

(27) Cotton, F. A.; Lin, C.; Murillo, C. A. *Inorg. Chem.* **2001**, *40*, 478.

(28) Chisholm, M. H.; Cotton, F. A.; Daniels, L. M.; Foltling, K.; Huffman, J. C.; Iyer, S. S.; Lin, C.; Macintosh, A. M.; Murillo, C. A. *J. Chem. Soc., Dalton Trans.* **1999**, 1387.

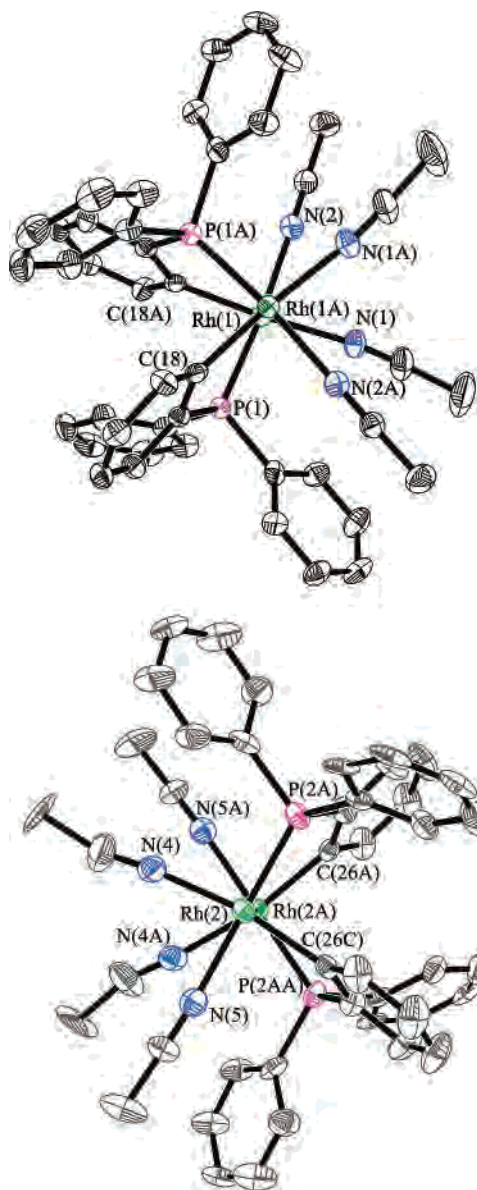


Figure 1. The cations in the racemic crystal of the precursor **1**. Displacement ellipsoids are drawn at the 40% probability level. All hydrogen atoms and axial acetonitrile ligands are omitted for clarity.

from acetonitrile molecules. The torsion angle is $-110.03(8)^\circ$ for $P(1)-Rh(1)-Rh(1A)-P(1A)$. The phosphine ligand on $Rh(2)$ is disordered in two positions with torsion angles of $116.2(3)^\circ$ for $P(2A)-Rh(2)-Rh(2A)-P(2AA)$ and $94.4(7)^\circ$ for $P(2B)-Rh(2)-Rh(2A)-P(2BA)$, respectively. Because compound **1** crystallizes in a centrosymmetric space group with the asymmetric unit containing a pair of *S* and *R* molecules, the composition of each crystal is racemic. The enantiomers have essentially identical dimensions, e.g., $Rh-Rh$ distances of 2.655(1) and 2.656(1) Å. The axial chain of $N_{ax}-Rh-Rh-N_{ax}$ deviates from linearity as indicated by the $Rh-Rh-N_{ax}$ angles of $\sim 170^\circ$, and this can be attributed to the steric requirements of the PPh_2 groups.

Within each of the two crystallographically independent dimetal units, there is torsional rotation of the two roughly square planes of equatorial ligands. The torsion angle of $-23.0(2)^\circ$ for $P(1)-Rh(1)-Rh(1A)-C(18)$ belongs to the molecule which does not show disorder in the phosphine

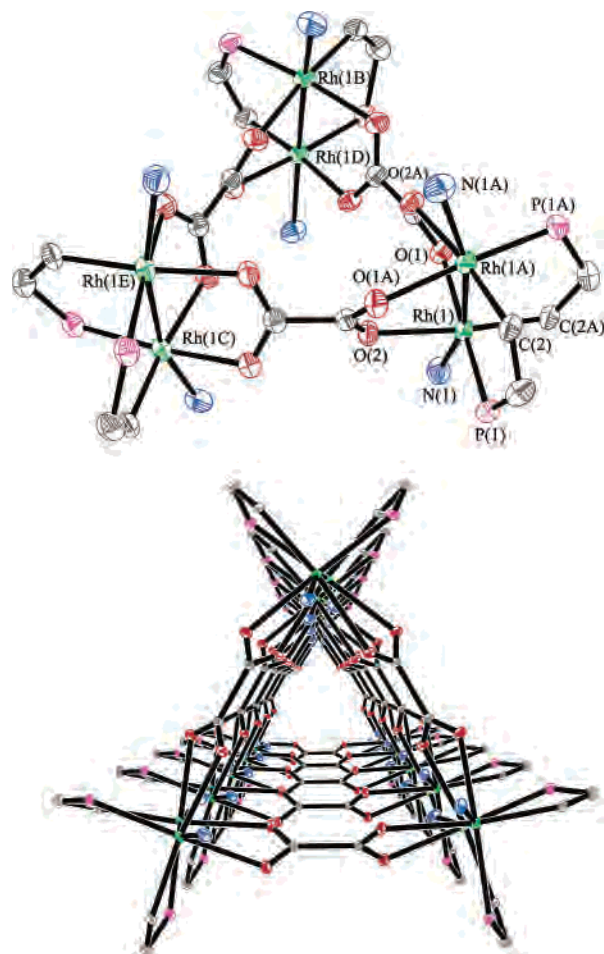


Figure 2. A drawing of the core of one of the enantiomers and packing pattern of **2**. Displacement ellipsoids of the atoms in the core are drawn at the 50% probability level. Some carbon atoms in the phosphine groups and pyridine ligands, solvent molecules, and hydrogen atoms have been omitted for clarity.

groups. For the $Rh_2(C_6H_4PPh_2)_2^+$ unit with disordered phosphine ligands, the torsion angles are $21.1(5)^\circ$ for $P(2A)-Rh(2)-Rh(2A)-C(26A)$ and $21(1)^\circ$ for $P(2B)-Rh(2)-Rh(2A)-C(26B)$. This rotation produces a helical conformation which introduces a second form of chirality to the molecules, and the conformers could be designated by the signs of the $P-R-R-C$ torsional angles according to commonly used nomenclature for helical molecules of *P* and *M*,²⁹ as shown in Scheme 4. Therefore, the chirality originating from the configurational relationship between the phosphine ligands, as defined by the $P-Rh-Rh-P$ torsion angles, is designated by the symbols *R* or *S*, whereas the chirality stemming from the conformational arrangement within each phosphine ligand in the molecule, as defined by the $P-Rh-Rh-C$ torsion angles, is designated by the symbols *P* or *M*. A complete description of the stereochemistry of the two independent

(29) In a helical system, *P* stands for plus and *M* for minus as they relate to the torsion angles along the axis of the helix. For the conformers in **1**, this axis coincides with the $Rh-Rh$ bond. See for example: (a) Cahn, R. S.; Ingold, C.; Prelog, V. *Angew. Chem., Int. Ed. Engl.* **1966**, *5*, 385. (b) Piguet, C.; Bernardinelli, G.; Hopfgartner, G. *Chem. Rev.* **1997**, *97*, 2005. (c) An, De L.; Nakano, T.; Orita, A.; Otera, J. *Angew. Chem., Int. Ed.* **2002**, *41*, 171. (d) Snatze, G. In *Chirality-From Weak Bosons to the α -Helix*; Janoschek, R., Ed.; Springer-Verlag: Berlin, 1991.

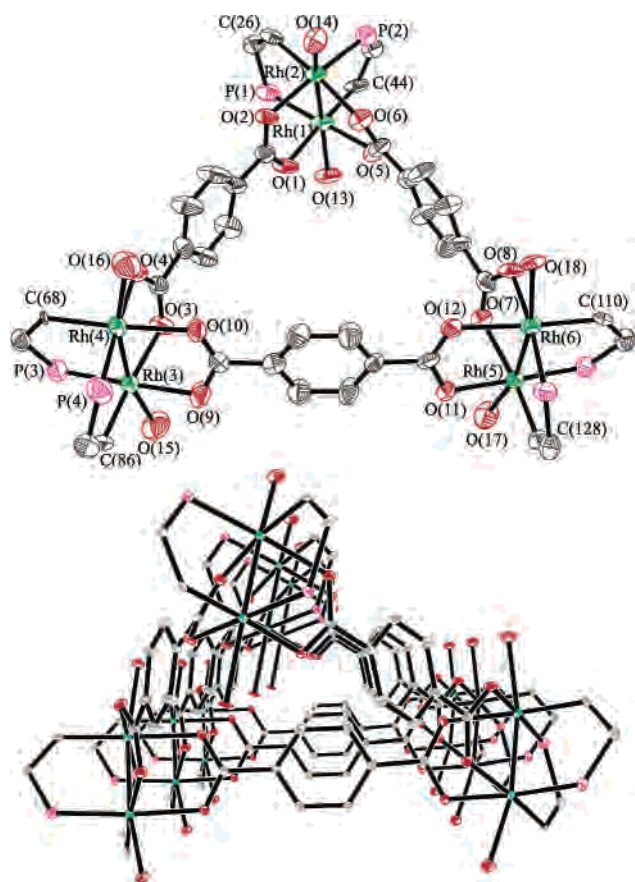
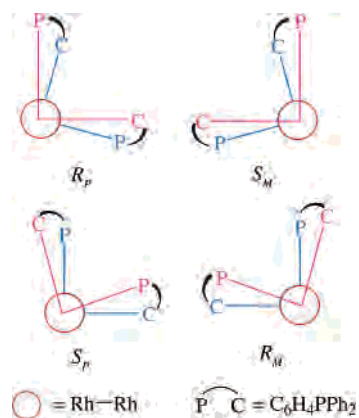


Figure 3. A drawing of the core and the packing pattern of **3**. Displacement ellipsoids for the core atoms are drawn at the 50% probability level. Some carbon atoms in the phosphine groups and the axially coordinated DMF ligands and interstitial solvent molecules and hydrogen atoms have been omitted for clarity.

Scheme 4



molecules in **1** requires specification of the two senses of chirality that can be represented as S_M and R_P .³⁰

It should be noted that the chirality induced by the conformational arrangement of the ligands (M or P) is only secondary when compared to the chirality (R or S) that arises from the configurational arrangement of the molecule. Interconversion of R and S is a process that requires a

(30) It should be noted that this nomenclature differs from that originally introduced for $cis\text{-Rh}_2(\text{C}_6\text{H}_4\text{PPh}_2)_2(\text{OAc})_2$ and its analogues in ref 18. We believe that our labeling system is more descriptive because it considers the two sources of chirality found in this type of molecule.

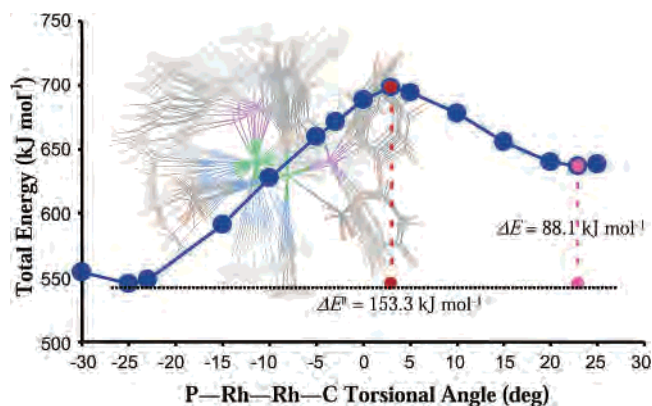


Figure 4. Variation of the minimized energy versus P–Rh–Rh–C angle for $S\text{-I}$. The inset shows the conformational changes of the molecule from S_M to S_P at various torsion angles.

chemical bond-breaking, and it should have a large energy barrier. This is consistent with the facile enantiomeric resolution of the parent $cis\text{-Rh}_2(\text{C}_6\text{H}_4\text{PPh}_2)_2(\text{OAc})_2$ molecule and the high stability of the enantiomers which do not racemize. Although less energy would be expected to be necessary for the interconversion between conformers, the relative value cannot be easily estimated by comparison with other molecules. Some helical conformers racemize easily, but others do not racemize.³¹ A similar contrast is found in the barriers to inversion for NH_3 and PH_3 which are 24 and 155 kJ mol^{-1} , respectively.³²

Molecular mechanics calculations (MMCs) have been performed to estimate the relative stability of the S_M and S_P molecules. The dimensions from the X-ray crystal structure for **1** were used as a starting point in the calculation. The initial structure of the $cis\text{-Rh}_2(\text{C}_6\text{H}_4\text{PPh}_2)_2(\text{MeCN})_6^{2+}$ ion in **1** has an S_M geometry with a P–Rh–Rh–C torsion angle of -23° . Minimization of the total energy was carried out by fixing the geometry of the inner core of the $cis\text{-Rh}_2(\text{C}_6\text{H}_4\text{PPh}_2)_2(\text{MeCN})_6^{2+}$ ion with C_2 symmetry, and then varying the torsion angle defined by the P–Rh–Rh–C unit from -30° to 25° in $2\text{--}5^\circ$ steps. All aryl groups and the acetonitrile carbon atoms were allowed to move freely during the energy minimization process.

A plot of minimized total energy at each calculated torsion angle is shown in Figure 4. The results show that the experimentally observed S_M conformation with a P–Rh–Rh–C twist angle of about -23° is preferred over the S_P structure with a 23° twist angle by 88.1 kJ mol^{-1} , and the energy barrier is estimated to be 153.3 kJ mol^{-1} . The increase in energy in going from the S_M to the S_P structure is mostly due to greater steric repulsions found at positive twist angles for the S enantiomer. Because the energy difference between conformers and the energy barrier for interconversion of conformers are much greater than the value of kT , the

(31) See for example: (a) Jiang, H.; Dolain, C.; Léger, J.-M.; Gornitzka, H.; Huc, I. *J. Am. Chem. Soc.* **2004**, *126*, 1034. (b) Gawronski, J.; Gawronska, K.; Grajewski, J.; Kacprzak, K.; Rychlewska, U. *Chem. Commun.* **2002**, 582. (c) Amendola, V.; Fabbrizzi, L.; Mangano, C.; Pallavicini, P. *Inorg. Chem.* **2000**, *39*, 5803. (d) See also ref 29c). (32) Cotton, F. A.; Wilkinson, G.; Murillo, C. A.; Bochmann, M. *Advanced Inorganic Chemistry*, 6th ed.; John Wiley & Sons: New York, 1999; p 383.

conformers are not expected to interconvert at ambient temperature.

Many structures containing Rh_2^{4+} units spanned by two orthometalated $\text{C}_6\text{H}_4\text{PAr}_2$ ligands have been reported since the first examples, $\text{Rh}_2(\text{C}_6\text{H}_4\text{PPh}_2)_2(\text{OAc})_2\text{L}_2$ ($\text{L} = \text{HOAc}$, py), were described in 1985.³³ In all cases where there have been two other bridging groups, the Rh–Rh distances have been in the range 2.49–2.77 Å. This is the first structurally characterized orthometalated Rh_2 compound in which the four additional equatorial positions are occupied by non-bridging ligands.

Because the *cis*- $\text{Rh}_2(\text{C}_6\text{H}_4\text{PPh}_2)_2^{2+}$ unit is inherently chiral, regardless of torsion angle, the molecular triangles based on this unit must also be chiral. In this work, we used a racemate of **1** as starting material to synthesize the target supramolecules. The combination of the racemic mixture of *cis*- $\text{Rh}_2(\text{C}_6\text{H}_4\text{PPh}_2)_2^{2+}$ units with dicarboxylate anions to form triangles can produce four possible stereoisomers: *RRR*, *RRS*, *SSR*, and *SSS*. Each of these can be either R_P and R_M , or S_P and S_M , and this increases the number of possible isomers. In **2**, all three Rh_2 units in each triangle have the same chirality, and this compound exists as a mixture of $R_P R_P R_P$ **2** and $S_M S_M S_M$ **2**. It is notable that we find only R_P and S_M conformers and we do not observe any R_M or S_P conformers. The unit cell contains 2 triangular molecules together with 12 methanol and 2 water molecules. Each triangle resides on a position of D_3 symmetry. Thus, only half of a Rh_2 unit is crystallographically independent, and the D_3 crystallographic symmetry generates the entire triangular molecule. The Rh–Rh distance is 2.5650(5) Å, and the Rh–N distance is 2.288(3) Å. The oxalate linkers are both bent and twisted about the central C–C bond. The significant twisting of the linker is indicated by the dihedral angle of 43.8° between the carboxylate groups of the oxalate bridge of 43.8°. The values of P–Rh–Rh–C and O–Rh–Rh–O angles are 12.7(1)° and 18.99(9)°, respectively. Within each Rh_2 unit, the P–Rh–Rh–P angle (105.31(5)°) is larger than that for the C–Rh–Rh–C unit (79.9(2)°), as in **1**.

In complex **3**, the Rh_2 units of the molecular triangles are linked by terephthalate groups, and all the axial positions are occupied by DMF ligands. There is a molecule of **3** on each of the four general positions in the monoclinic space group $P2_1/n$; the entire molecular triangle is the asymmetric unit. Unlike the triangles with oxalate linkers in which the three Rh_2 units have the same chirality ($R_P R_P R_P$ or $S_M S_M S_M$),

in **3** each molecule contains two Rh_2 units of one chirality (Rh1–Rh2 and Rh5–Rh6 as shown in Figure 3) and one Rh_2 unit of the other chirality (Rh3–Rh4), but in all cases the *R* isomers correspond to R_P and the *S* to S_M . The molecular structure has idealized C_2 symmetry with the 2-fold axis through the midpoint of the Rh3–Rh4 bond. The Rh–Rh bond distances of 2.514(1), 2.507(1), and 2.511(1) Å are slightly shorter than those in **2**, which is consistent with the difference in the electronic donating ability of the py and DMF axial ligands. The axial Rh–O distances, in the range from 2.285(7) to 2.335(9) Å, and the other distances are normal. The torsion angle P–Rh–Rh–P in each Rh_2 unit is again larger than the accompanying C–Rh–Rh–C angle. Like the oxalate linkers in **2**, the terephthalate dianions in **3** are not flat: the carboxylate groups make angles between 7(1)° to 26(1)° with the C_6H_4 ring-plane and angles in the range 4(1)–39(1)° with each other.

The quality of the diffraction data³⁴ for **4** was insufficient for a detailed structural analysis. However, it unambiguously shows the existence of a triangle composed of three equivalent *cis*- $\text{Rh}_2(\text{C}_6\text{H}_4\text{PPh}_2)_2(\text{py})_2^{2+}$ units and three 4,4'-diphenyl-dicarboxylate dianions. Because of crystallographic disorder, each Rh_2 site consists of equal amounts of the *R* and *S* enantiomeric forms, but it is impossible to distinguish from the crystal structure whether the molecules are *RRS*, *SSR* or *RRR*, *SSS*. Fortunately, NMR spectroscopy has been able to elucidate this issue, as explained below.

The molecular structures of **2–4** can each be described as an equilateral triangle consisting of three singly bonded orthometalated [*cis*- $\text{Rh}_2(\text{C}_6\text{H}_4\text{PPh}_2)_2$]²⁺ components linked by two dicarboxylate dianions. The edges of the triangles are about 6.80, 11.10, and 15.40 Å for **2**, **3**, and **4**, respectively. The packing patterns of these molecular triangles are also interesting. In **2** and **4**, the triangular molecules stack directly on top of each other creating triangular channels in the crystal. The packing pattern of **3** is different as the molecular triangles stack on top of each other but not directly because of tilting of the molecules. However, this also results in the formation of small channels, and these are filled with disordered DMF molecules.

In each of the triangular molecules the two axial positions of each Rh_2 unit are occupied by py or DMF molecules. As for **1**, the $\text{L}_{\text{ax}}\text{-Rh-Rh-L}_{\text{ax}}$ entities deviate significantly from linearity as indicated by their Rh–Rh–O(or N) angles, which are all in the range 160–165°. If the axial ligands are better electron donors, the Rh–Rh distances are ca. 0.05 Å longer than those with poorer electron donors. The distances of Rh– L_{ax} are ~2.26 Å for Rh–N (pyridine) and ~2.35 Å for Rh–O (DMF). Other distances such as Rh–C, Rh–P, and Rh–O in equatorial positions are as expected.

(33) (a) Barceló, F.; Cotton, F. A.; Lahuerta, P.; Sanaú, M.; Schwotzer, W.; Ubeda, M. A. *Organometallics* **1987**, *6*, 1105. (b) Lahuerta, P.; Martínez-Mañez, R.; Paya, J.; Peris, E. *Inorg. Chim. Acta* **1990**, *173*, 99. (c) Morrison, E. C.; Tocher, D. A. *J. Organomet. Chem.* **1991**, *408*, 105. (d) Lahuerta, P.; Payá, J.; Peris, E.; Aguirre, A.; García-Granda, S.; Gómez-Beltrán, F. *Inorg. Chim. Acta* **1992**, *192*, 43. (e) Borrachero, M. V.; Estevan, F.; García-Granda, S.; Lahuerta, P.; Latorre, J.; Peris, E.; Sanaú, M. *Chem. Commun.* **1993**, 1864. (f) Estevan, F.; Lahuerta, P.; Peris, E.; Ubeda, M. A.; García-Granda, S.; Gómez-Beltrán, F.; Pérez-Carreño, E.; González, G.; Martínez, M. *Inorg. Chim. Acta* **1994**, *218*, 189. (g) Estevan, F.; García-Granda, S.; Lahuerta, P.; Latorre, J.; Peris, E.; Sanaú, M. *Inorg. Chim. Acta* **1995**, *229*, 365. (h) Lahuerta, P.; Pereira, I.; Pérez-Prieto, J.; Sanaú, M.; Stiriba, S.-E.; Taber, D. F. *J. Organomet. Chem.* **2000**, *612*, 36. (i) Estevan, F.; Krueger, P.; Lahuerta, P.; Moreno, E.; Pérez-Prieto, J.; Sanaú, M.; Werner, H. *Eur. J. Inorg. Chem.* **2001**, 105.

(34) Crystallographic data for **4**: $a = 27.697(2)$ Å, $b = 27.697(2)$ Å, $c = 20.855(3)$ Å, $\alpha = 90^\circ$, $\beta = 90^\circ$, $\gamma = 120^\circ$, $V = 13855(2)$ Å³, space group $P31c$, R1 and wR2 = 0.1367 and 0.3510. The Rh–Rh distance is 2.541(3) Å, and the P–Rh–Rh–P torsion angle is larger than respective C–Rh–Rh–C angles. Compared to **2** and **3**, the Rh_2 units in **4** appear closer to having an eclipsed structure. The average of C–Rh–Rh–P is 9.0°. The value of 0.6° for the O–Rh–Rh–O angle is very close to that in an eclipsed species.

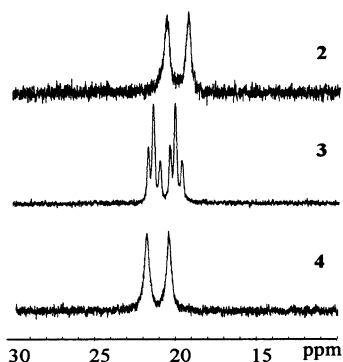


Figure 5. ^{31}P NMR in CDCl_3 of the triangular compounds **2**, **3**, and **4** with chemical shifts referenced to H_3PO_4 .

The question of why **2** and **4** consist of *RRR* and *SSS* molecules, while **3** consists of *RRS* and *SSR* molecules, is not easy to answer with certainty. It may be that in **2** the short distance between Rh_2 moieties means that each one requires its neighbors to be the same in order for all of them to fit.

NMR Spectroscopy. This technique provides information concerning the molecular structure in solution. For simplicity, and because the structural studies show the presence of only R_P and S_M isomers, we will use the simplified nomenclature of *R* and *S* to describe the isomers in the following discussion. As already mentioned, the combination of the racemic $[\text{cis-Rh}_2(\text{C}_6\text{H}_4\text{PPh}_2)_2]^{2+}$ unit with achiral linear linkers might produce four possible stereoisomers of triangles, i.e., *RRR*, *RRS*, *SSR*, and *SSS*. Each Rh_2 unit also has two labile axial ligands such as acetonitrile or pyridine molecules. If all of the axial sites are the same, the *RRR* and *SSS* isomers have D_3 symmetry, and thus all six orthometalated phosphine ligands will be equivalent, and the ^{31}P NMR spectrum must show only a single signal, which will be a doublet due to coupling of the P atom to the $I = 1/2$ ^{103}Rh nucleus. The *RRS* and *SSR* isomers have C_2 symmetry, and their ^{31}P NMR spectrum should show three doublets. If squares were to form in solution, there would be six possible combinations, i.e., *RRRR*, *RRRS*, *RRSS*, *RSRS*, *RSSS*, and *SSSS*. The symmetry of the *RRRR* (or *SSSS*), *RRRS* (or *SSSR*), *RRSS*, and *RSRS* isomers are D_4 , C_2 , C_{2h} , and D_2 , respectively, so their ^{31}P NMR spectra should show only one doublet for *RRRR* (or *SSSS*), four doublets for *RRRS* (or *SSSR*), or two doublets for *RRSS* and *RSRS*. If there were an equilibrium between triangular and square species in solution, the spectrum would be much more complex.

The ^{31}P NMR spectra for all triangular compounds are shown in Figure 5. That of **2** in CDCl_3 appears as a sharp doublet,³⁵ indicating there is only one highly symmetric species in solution. This is consistent with the high symmetry revealed by the crystal structure of **2** in which the molecules exist as *RRR* and *SSS* isomers. However, it is expected that the ^{31}P NMR spectra of square molecules (*RRRR* or *SSSS*

(35) In general, the ^{31}P $\{^1\text{H}\}$ NMR signals were sharp when a strongly coordinating solvent such as pyridine or DMF was added to the solution. The signals were broader when mixtures of weaker coordinating solvents, e.g., MeOH and H_2O , were present in the NMR solvent.

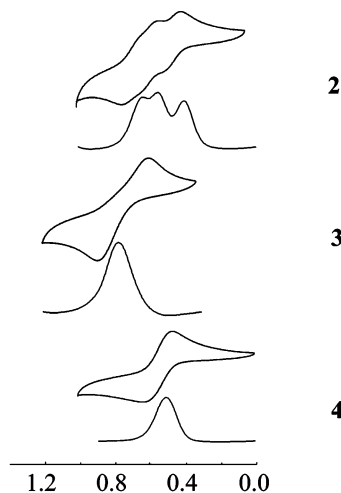


Figure 6. Cyclic voltammograms and differential pulse voltammograms (below each CV) for **2–4**. Each was recorded in CH_2Cl_2 , and potentials are referenced in the Ag/AgCl electrode.

isomers) also show only a sharp doublet. Strictly speaking, in this case it is not possible to tell whether the compound exists in solution as a triangle or a square from the ^{31}P NMR spectrum. Fortunately, positive ion electrospray ionization mass spectrometry (+ESI-MS) has proven valuable in showing the existence and retention of the identity of supramolecules in solution. The ESI spectrum of **2** in CH_2Cl_2 shows only molecular triangles and has signals that correspond to doubly charged molecular ions centered at $m/z = 1389.51$, 1349.98 , and 1310.45 amu that can be attributed to $\{[\text{Rh}_2(\text{C}_6\text{H}_4\text{PPh}_2)_3(\text{C}_2\text{O}_4)_3(\text{py})_m(\text{H}_2\text{O})]^{2+}\}$ ($m = 4, 3$, and 2 , respectively). Because these signals correspond to doubly charged ions, they occur at an amu value of half the mass of the triangle. These signals can be attributed unambiguously to $2+$ ions because the proper isotopic distribution pattern expected for the molecule is seen, but the peaks are separated by a value of 0.5 amu.

In contrast to that of **2**, the ^{31}P NMR spectrum of **3** in CDCl_3 in the presence of DMF has three doublets with nearly identical coupling parameters of 165.3 , 165.8 , and 166.2 Hz. This is consistent with the above analysis of the triangle with *RRS* or *SSR* chirality, which is found in the crystal structure, but is not consistent with any of the possibilities for molecular squares. Therefore, it is reasonable to conclude that there are no molecular squares in the solution of **3**.

From the X-ray structure of **4**, the chirality of the molecular triangle could not be determined because of the disorder of the phosphine ligands, but its ^{31}P NMR spectrum consists of only a sharp doublet indicating that there is only a highly symmetric species in solution. This rules out the possibility of *RRS* and *SSR* isomers, but is consistent with a mixture of *RRR* and *SSS* isomers. The MS spectra of **3** and **4** indicate that these two supramolecules are not stable under the ionization conditions, and only fragments from these molecules have been observed.

Electrochemistry. Compounds **1–4** have been studied both by cyclic voltammetry (CV) and differential pulse voltammetry (DPV). The results are summarized in Figure 6 and Table 5. The CV of the dinuclear complex **1** in CH_2Cl_2

Table 5. Electrochemical Data^a for **1–4** in CH₂Cl₂

compd	$E_{1/2}$ (V)
1 ^b	1.412
2 ^{b,c}	0.420, 0.563, 0.682
3 ^d	0.805
4 ^{c,d}	0.585

^a All potentials are referenced to Ag/AgCl, and under the present conditions, the $E_{1/2}(\text{Fc}^+/\text{Fc})$ was consistently measured at 440 mV. ^b $E_{1/2} = (E_{\text{pa}} + E_{\text{pc}})/2$. ^c 0.20 mL of pyridine was added. ^d $E_{1/2} = E_{\text{p}} + E_{\text{pul}}/2$, $E_{\text{pul}} = 50$ mV.

Cl₂ is simple and shows a one-electron redox process at $E_{1/2} = 1.412$ V which is assigned to the Rh₂⁴⁺/Rh₂⁵⁺ couple. However, the electrochemical behavior of **2–4** is more complex than that of **1**. For the triangles, there are three redox-active Rh₂⁴⁺ units, and electronic coupling between the Rh₂⁴⁺ units affects the separation of the half wave potentials ($E_{1/2}$) to different extents. The CV of **2** shows three redox waves at $E_{1/2} = 0.420$, 0.563, and 0.682 V which correspond to the redox couples {Rh₂}₃¹²⁺/ {Rh₂}₃¹³⁺, {Rh₂}₃¹³⁺/ {Rh₂}₃¹⁴⁺, and {Rh₂}₃¹⁴⁺/ {Rh₂}₃¹⁵⁺, respectively. For **3** and **4**, the DPVs show a simpler pattern having only one broad signal centered at 0.805 and 0.585 V, respectively. Clearly, the higher degree of electronic coupling between the Rh₂⁴⁺ units, seen in **2** because of the short oxalate linkers, is largely lost in **3** and **4** because the linkers are very long.

It should be noted that the electrochemical profiles of all of these new triangles are indefinitely stable, whereas that of the other known Rh₂⁴⁺ molecular triangle, [Rh₂(*cis*-DAniF)₂(O₂CCO₂)₃], changes slowly over a period of several

hours.^{6a} This is because an equilibrium between the triangle and the square species [Rh₂(*cis*-DAniF)₂(O₂CCO₂)₄] is established in solution. The electrochemical data for **2–4** show that there are no such equilibria in these solutions.

Concluding Remarks. The preparation and structure of the racemic dirhodium compound *cis*-[Rh₂(C₆H₄PPh₂)₂(CH₃-CN)₆](BF₄)₂ (**1**) is described, and its use to synthesize triangular supramolecules by reaction with rigid linear dicarboxylate salts is presented. Single crystal structural analysis, NMR spectrum, mass spectrometry, and electrochemical studies of the resulting supramolecules have indicated that in each case there are molecular triangles (and only triangles) in both the solid state and in solution.

This work is the first step in an effort to make catalysts and molecular sensors based on chiral metal components of supramolecular compounds. The use of these triangles to catalyze the decomposition of diazo compounds will be investigated, and studies designed to make enantiopure triangles are underway.

Acknowledgment. We thank the National Science Foundation for financial support and Dr. J. F. Berry for helpful discussions. We also thank Johnson-Matthey for the generous loan of rhodium trichloride.

Supporting Information Available: X-ray crystallographic data in CIF format for **1**, **2**, and **3** and a plot in PDF of **4** drawn from crystallographic data. This material is available free of charge via the Internet at <http://pubs.acs.org>.

IC0492183